Electronic Supplementary Material (ESI) for Lab on a Chip.

Supplementary Information

Design of highly robust super-liquid-repellent surfaces that can resist high-velocity impact of low-surface-tension liquids

Yingke Wang,‡[ab] Yue Fan,‡[ab] Hongtao Liu,[ab] Shuai Wang,[ab] Lin Liu,[b] Yingying Dou,*[ab] Shilin Huang,[ab] Juan Li,*[abc] Xuelin Tian*[ab]

[a]School of Materials Science and Engineering, Key Laboratory for Polymeric Composite & Functional Materials of Ministry of Education, Guangzhou Key Laboratory of Flexible Electronic Materials and Wearable Devices, Sun Yat-sen University, Guangzhou 510006, China

[b]State Key Laboratory of Optoelectronic Materials and Technologies, Sun Yat-sen University, Guangzhou 510006, China

[c]School of Traditional Chinese Medicine Resources, Guangdong Pharmaceutical University, Guangzhou 510006, China

‡Co-first authors

*Corresponding author at: School of Materials Science and Engineering, Sun Yat-sen University, Guangzhou 510006, China

E-mail addresses: douyy5@mail.sysu.edu.cn (Y. Dou)
juanli@gdpu.edu.cn (J. Li)
tianxuelin@mail.sysu.edu.cn (X. Tian)

Theoretical calculation of apparent contact angle and robustness Factor

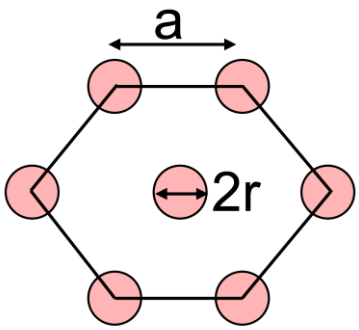

Fig. S1 Schematic showing the hexagonal array of doubly reentrant posts used in the modelling, in which r is the post radius and a is the post-post distance.

A hexagonal array of doubly reentrant posts shown in Figure S1 is used for modelling. For simplification purpose, the effect of the side wall of the doubly reentrant posts on θ^* is neglected, and the apparent contact angle θ^* of the textured surface can be given by the Cassie-Baxter equation[1]:

$$\cos\theta^* = \phi_s(\cos\theta_0+1)-1 \quad (1)$$

where ϕ_s solid-liquid contact area fraction, and θ_0 is the intrinsic contact angle. In our modelling, θ_0 is set as 60° considering that most fluorinated coatings have θ_0 close to this value for common oils. The solid-liquid contact fraction ϕ_s is calculated to be:

$$\phi_s = \frac{3\pi r^2}{\frac{3}{2}\sqrt{3}\,a^2} \quad (2)$$

Accordingly, the post radius can be expressed as:

$$r = \sqrt{\frac{\sqrt{3}\,\phi s}{2\pi}}*a \quad (3)$$

The critical breakthrough pressure of liquids on the nano-doubly-reentrant structures depends on the ratio of $F_{capillary}$ to $S_{l\text{-}g}$, where $F_{capillary}$ is the upward capillary force generated at the solid-liquid-gas triple contact line and $S_{l\text{-}g}$ is the projection area of liquid-gas contact area. For the hexagonal repeating unit in Figure 1a, $F_{capillary}$ is equal to $\gamma*3*2\pi$ (γ is the liquid surface tension), considering that the doubly reentrant posts can maximize the upward component of the capillary force, and the projected liquid-gas contact area is given by: $\frac{3}{2}\sqrt{3}\,a^2 - 3\pi r^2$.Therefore, we can get the critical breakthrough pressure and express as it a function of ϕ_s:

$$P_{cric} = \frac{\gamma*3*2\pi r}{\frac{3}{2}\sqrt{3}\,a^2-3\pi r^2} = \frac{\gamma*3*2\pi\sqrt{\frac{\sqrt{3}\,\phi s}{2\pi}}*a}{\frac{3}{2}\sqrt{3}\,a^2-3\pi\frac{\sqrt{3}\,\phi s*a^2}{2\pi}} = \frac{2\gamma\sqrt{\frac{\sqrt{3}\,\phi s*\pi}{2}}}{\frac{\sqrt{3}}{2}a(1-\phi s)} \quad (4)$$

The interface robustness factor is given by: $RF = P_{cric}/P_{ref}$, and the reference pressure P_{ref} equals $2\gamma/l_{cap}$, in which l_{cap} is the capillary length $l_{cap} = \sqrt{\gamma/\rho g}$, ρ the liquid density and g the gravity acceleration[2]. In our modelling, the surface tension γ is set as 10 mN/m and the liquid density ρ is 1000 kg/m^3. Accordingly, the robustness factor is given as:

$$RF = \frac{\text{Pcric}}{\text{Pref}} = \frac{\frac{\gamma*3*2\pi r}{\frac{3}{2}\sqrt{3}\,a^2 - 3\pi r^2}}{\frac{2\gamma}{\sqrt{\frac{\gamma}{\rho g}}}} \quad (5)$$

Substitute Eq. 3 into Eq. 5, the robustness factor is rewritten as:

$$RF = \frac{\frac{\gamma*3*2\pi\sqrt{\frac{\sqrt{3}\,\phi s}{2\pi}}*a}{\frac{3}{2}\sqrt{3}\,a^2 - 3\pi\frac{\sqrt{3}\,\phi s*a^2}{2\pi}}}{\frac{2\gamma}{\sqrt{\frac{\gamma}{\rho g}}}} \quad (6)$$

Simplifying the above equation gives the robustness factor as follows:

$$RF = \frac{\sqrt{\frac{\sqrt{3}\,\phi s*\pi}{2}}}{\frac{\sqrt{3}}{2}a(1-\phi s)} * \sqrt{\frac{\gamma}{\rho g}} \quad (7)$$

From Eqs. (1) and (7), we can calculate the apparent contact angle θ^* and robustness factor *RF* as functions of the solid-liquid contact fraction ϕ_s, as shown in Figure 1b.

From Eq. (1), it follows that:

$$\phi_s = \frac{\cos\theta* + 1}{\cos\theta_0 + 1} = \frac{2}{3}(\cos\theta^* + 1) \quad (8)$$

Substitute Eq. (8) into Eq. (7), the relationship between *RF* and θ^* can be obtained:

$$RF = \frac{\sqrt{\frac{\sqrt{3}\frac{2}{3}(\cos\theta* + 1)*\pi}{2}}}{\frac{\sqrt{3}}{2}a\left(1-\frac{2}{3}(\cos\theta* + 1)\right)} * \sqrt{\frac{\gamma}{\rho g}} \quad (9)$$

Further simplification gives the following equation:

$$RF = \frac{2\sqrt{\sqrt{3}(\cos\theta* + 1)*\pi}}{a*(1-2\cos\theta*)} * \sqrt{\frac{\gamma}{\rho g}} \quad (10)$$

From Eq. (10), we can calculate the relationship between *RF* and θ^* for different structural unit sizes as shown in Figure 1c.

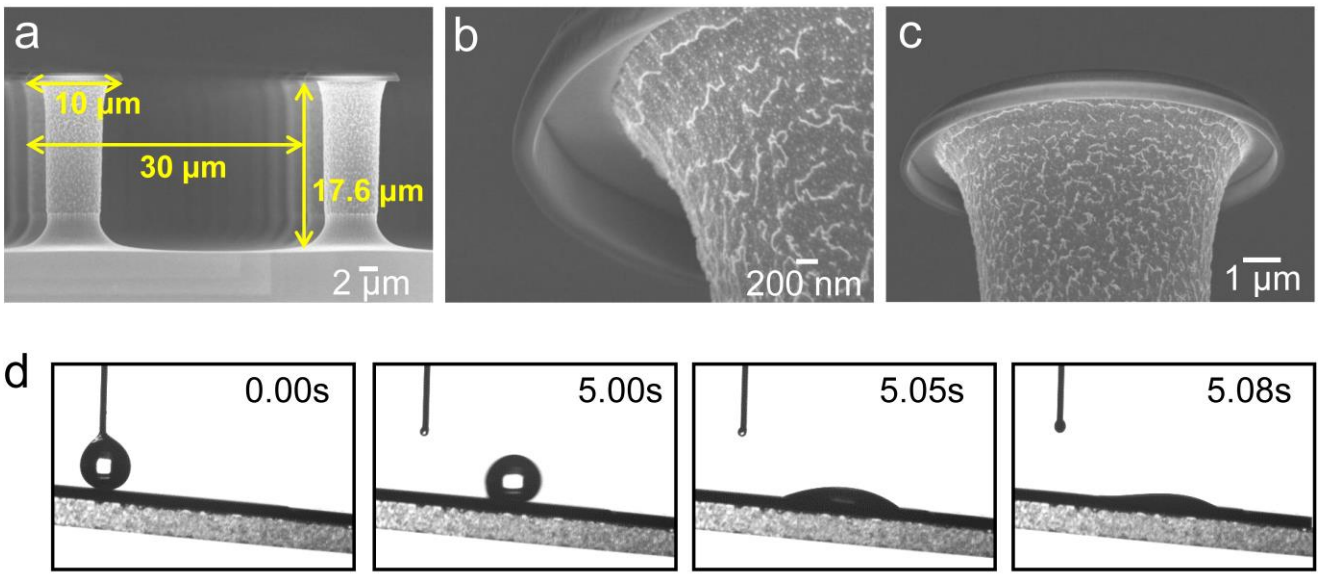

Fig. S2 (a-c) SEM images of a surface made of microscale doubly reentrant posts (diameter 10 µm, pitch 30 µm). (d) An ethanol droplet rolling on the surface tends to collapse and impale into the textures.

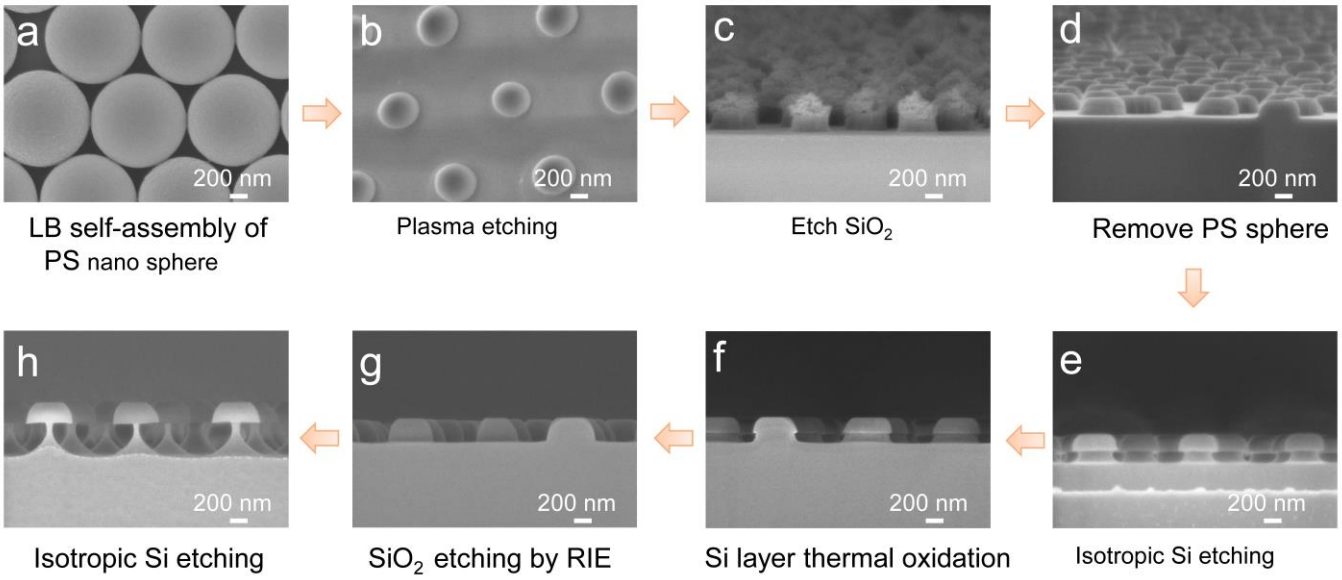

Fig. S3 SEM images showing the fabrication process of the NDR structures.

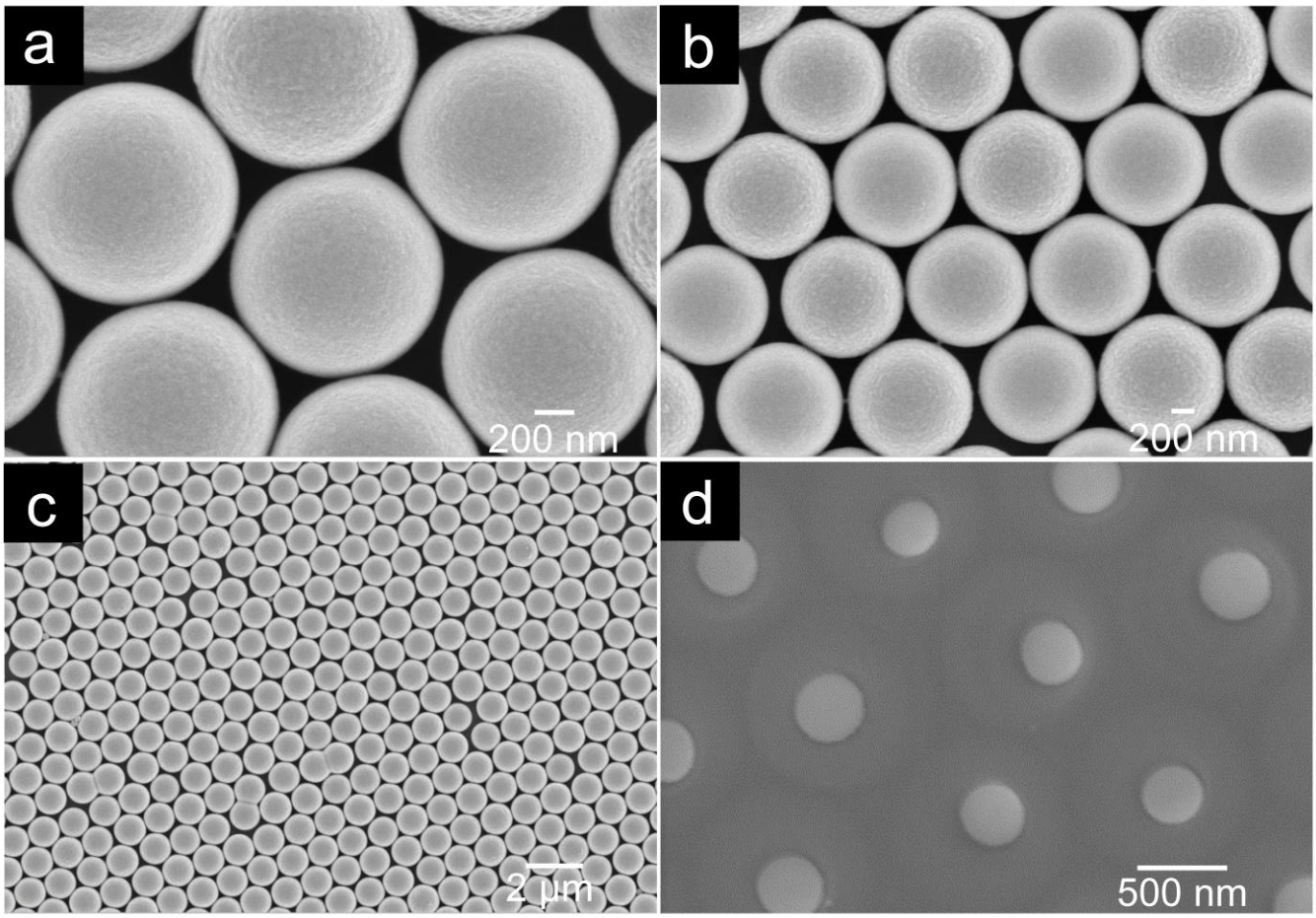

Fig. S4 (a-c) Hexagonally densely arranged polystyrene spheres by Langmuir-Blodget self-assembly. (d) Polystyrene nano-mask plate obtained after a reactive ion etching.

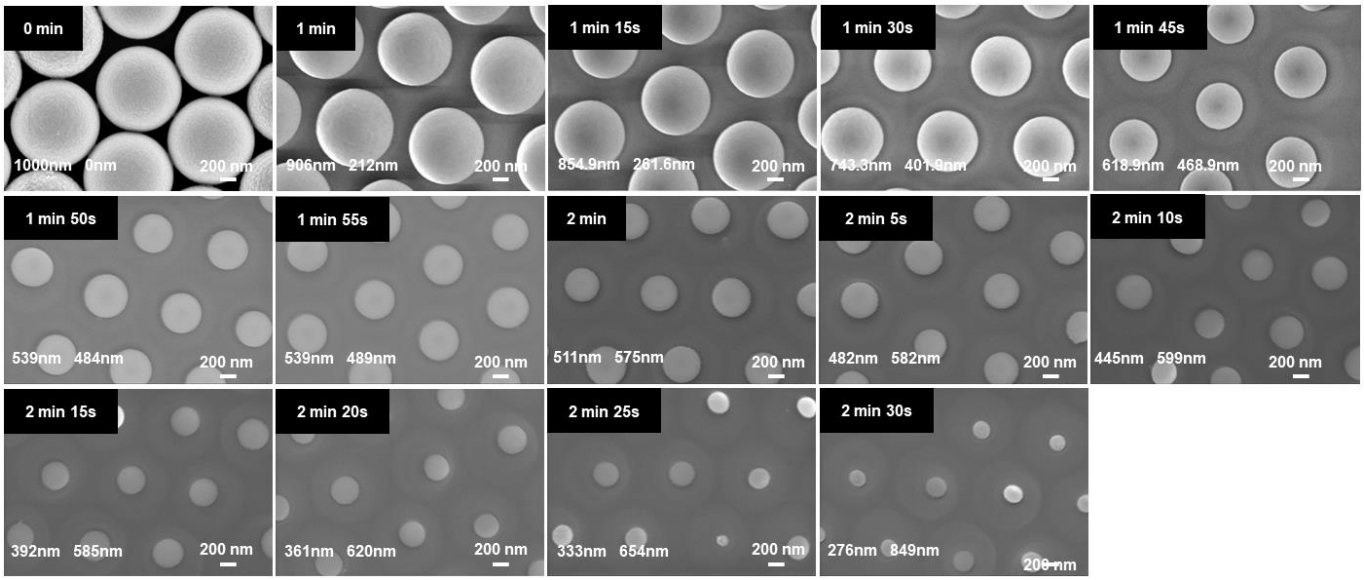

Fig. S5 Variation of the size and morphology of polystyrene microspheres with etching time. It was found that the size of the polystyrene spheres gradually decreased and the spacing between the spheres increased with the etching time. However, when the etching time increased to 2 min 25 s, the polystyrene nanospheres were not be able to maintain a good mask structure. Therefore, the optimal etching time was found to be 2 min 20 s for the preparation of nanoscale doubly structures with a low solid fraction.

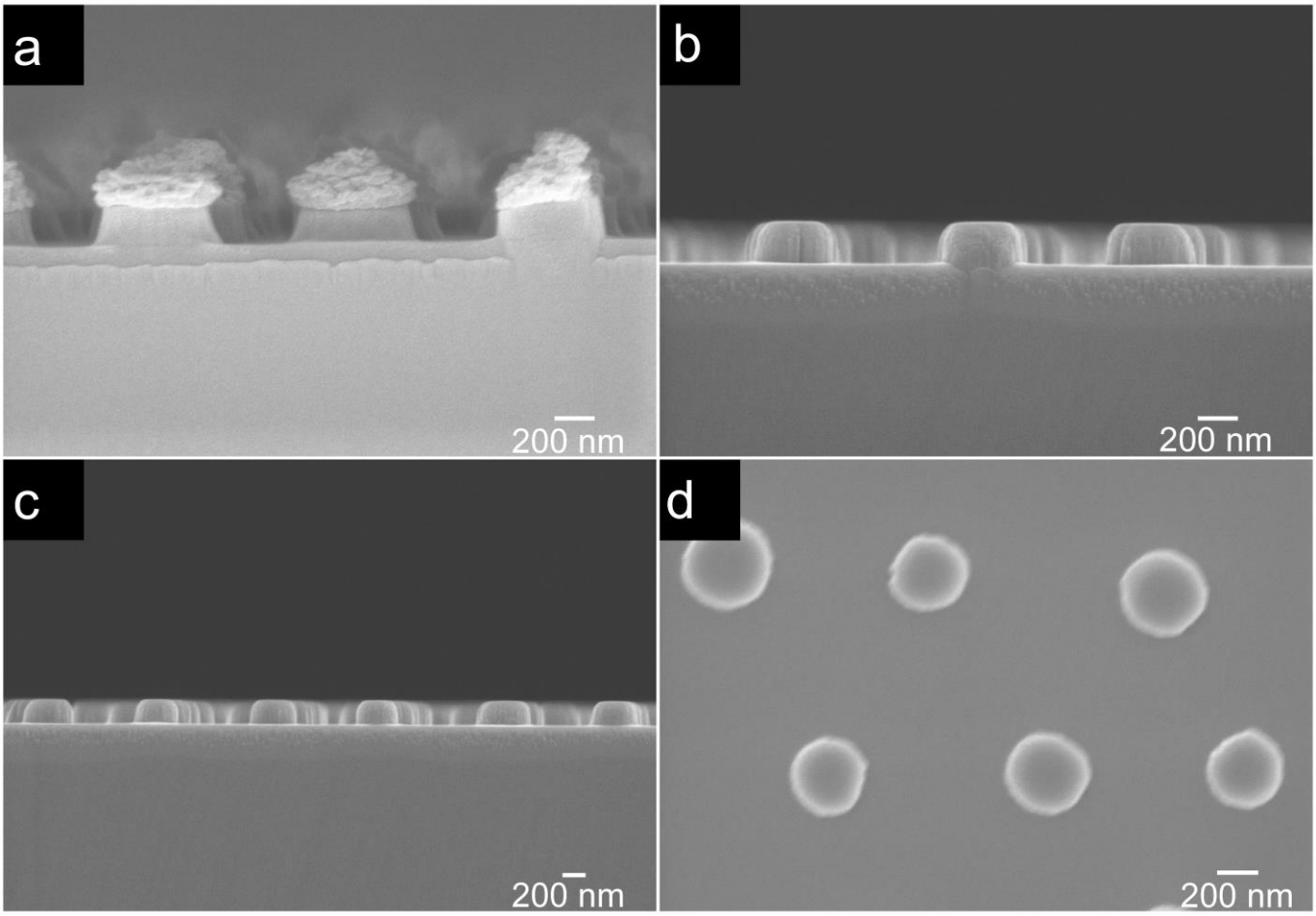

Fig. S6 (a) Polystyrene nano-mask transferred to the silica layer by SiO_2 etching. (b-c) Cross-section and (d) top views of silica nano-mask plate after removal of residual polystyrene spheres.

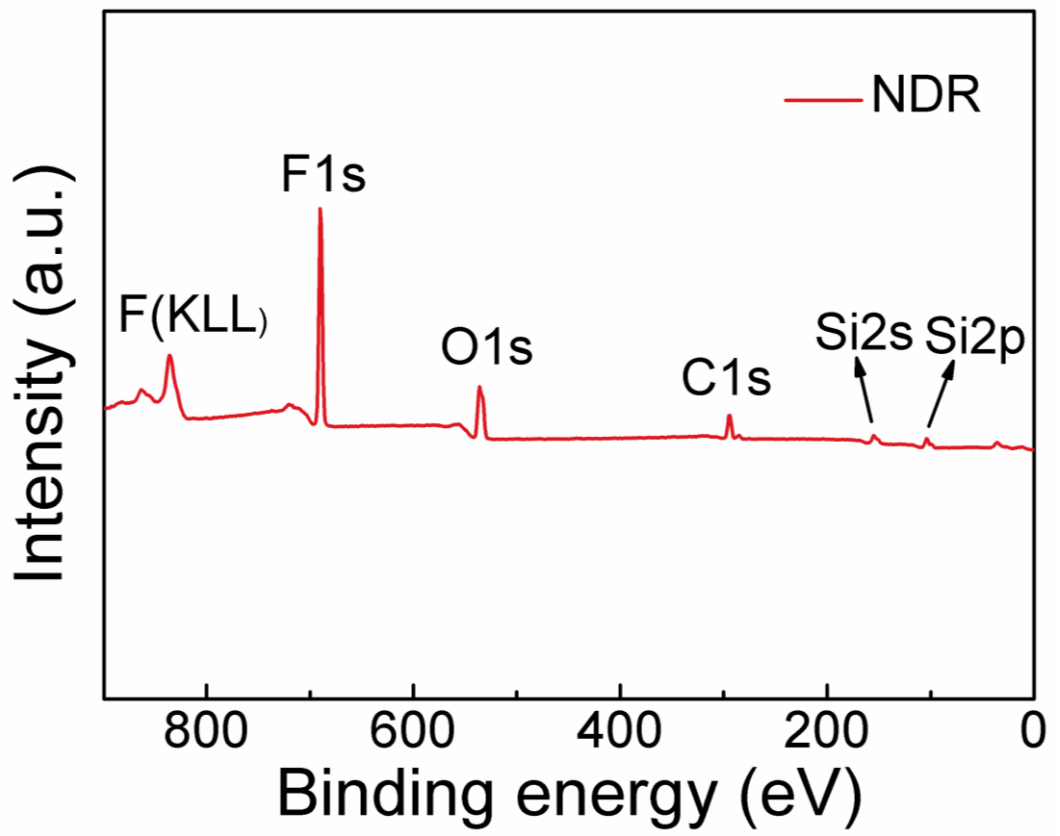

Fig. S7 XPS spectra of the NDR surfaces, showing the successful surface modification of the sample with PFPE.

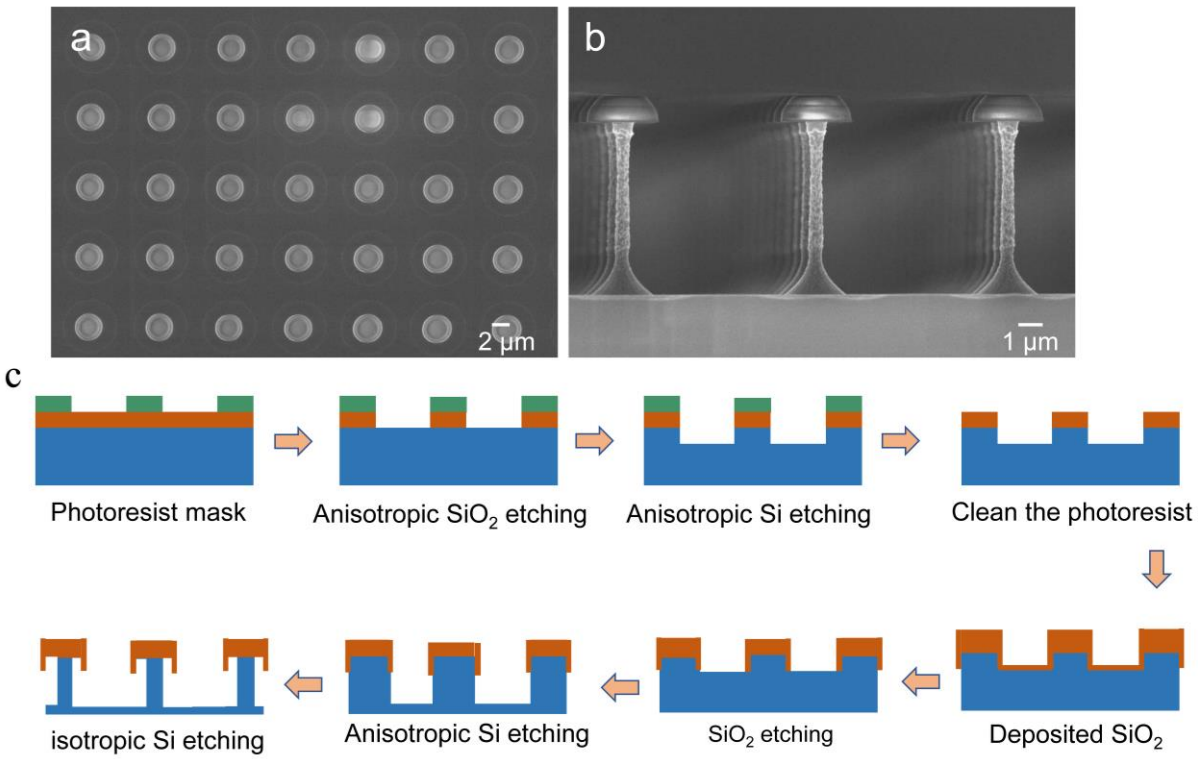

Fig. S8 (a) Top and (b) cross-section view images of the control sample composed of microscale doubly reentrant (MDR) posts. (c) Schematic showing the fabrication process of the MDR surface.

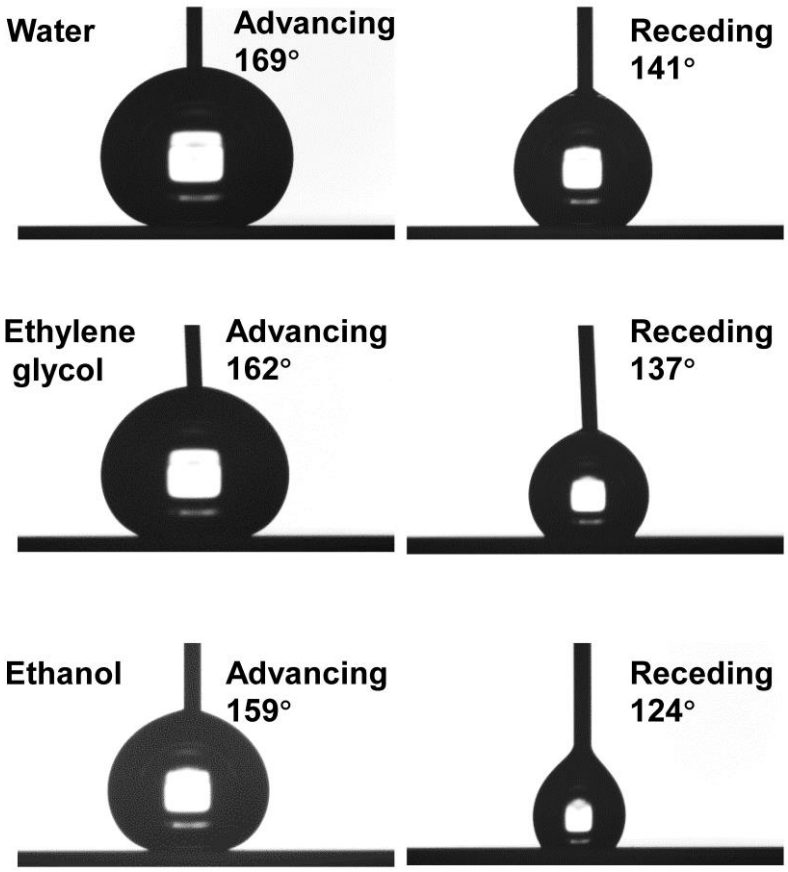

Fig. S9 Photos showing the advancing and receding contact angles of the control MDR surface for water, ethylene glycol and ethanol.

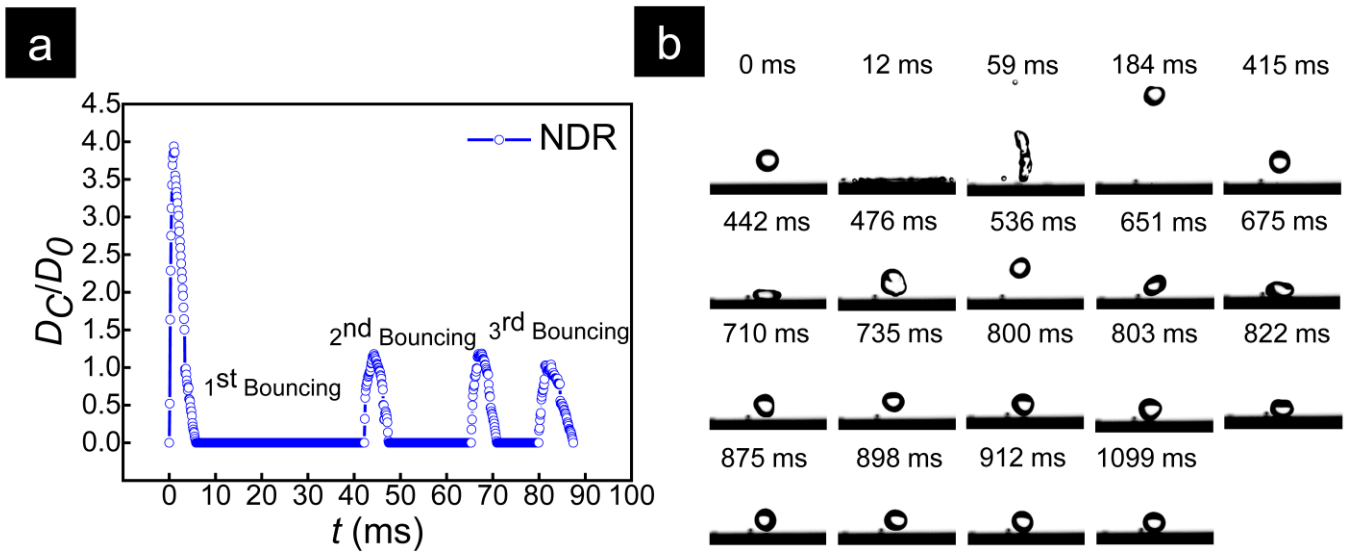

Fig. S10 (a) Temporal evolution of the normalized contact diameter and (b) snapshots showing multiple bounces of a water drop on the NDR surface (*We* ~ 257).

Recipes for the preparation of the NDR surface

Table S1 Recipe 1 for polystyrene etching by RIE

O_2 (sccm)	CF_4 (sccm)	Set Pressure (W)	Forward Power (W)	DC Bias (V)	Chamber Temperature (Deg)	Helium Pressure (Torr)	Etching Time (s)
30	20	30	100	495	20	8	140

Table S2 Recipe 2 for SiO_2 etching by RIE

Ar (sccm)	CHF_3 (sccm)	Set Pressure (W)	Forward Power (W)	DC Bias (V)	Chamber Temperature (Deg)	Helium Pressure (Torr)	Etching Time (min)	Etching Thickness (nm)
38	12	30	200	767	20	10	4.5	200

Table S3 Recipe 3 for anisotropic Si etching by ICP

HBr (sccm)	ICP Power (W)	Set Pressure (W)	Forward Power (W)	DC Bias (V)	Chamber Temperature (Deg)	Helium Pressure (Torr)	Etching Time (s)	Etching Thickness (nm)
20	500	4	57	166	20	10	20	40

Table S4 Recipe 4 for isotropic Si etching by RIE

SF_6 (sccm)	Set Pressure (W)	Forward Power (W)	DC Bias (V)	Chamber Temperature (Deg)	Helium Pressure (Torr)	Etching Time (s)	Etching Thickness (nm)
100	50	100	289	20	10	7	51

Table S5 Recipe 5 for SiO_2 etching by RIE

Ar (sccm)	CHF_3 (sccm)	Set Pressure (W)	Forward Power (W)	DC Bias (V)	Chamber Temperature (Deg)	Helium Pressure (Torr)	Etching Time (s)	Etching Thickness (nm)
38	12	30	200	767	20	10	165	100

Table S6 Recipe 6 for isotropic Si etching by ICP

SF_6 (sccm)	O_2 (sccm)	ICP Power (W)	Set Pressure (W)	Forward Power (W)	Chamber Temperature (Deg)	Helium Pressure (Torr)	Etching Time (s)	Etching Thickness (nm)
30	10	500	8	30	20	6	10	370

Recipes for the preparation of the MDR surface

Table S7 Recipe 7 for anisotropic SiO_2 etching by DRIE

C_4F_8 Flux (sccm)	Ar Flux (sccm)	ICP Power (W)	Forward Power (W)	APC Pressure (mTorr)	Chamber Temperature (Deg)	Helium Pressure (Torr)	Etching Time (min)	Etching Depth (μm)
15	45	1000	100	30	20	10	5.5	1

Table S8 Recipe 8 for anisotropic Si etching by ICP

HBr (sccm)	ICP Power (W)	Set Pressure (W)	Forward Power (W)	DC Bias (V)	Chamber Temperature (Deg)	Helium Pressure (Torr)	Etching Time (min)	Etching Depth (nm)
20	500	4	57	166	20	10	2	480

Table S9 Recipe 9 for deposition SiO_2 by ICP180-CVD

N_2O (sccm)	SiH_4 (sccm)	ICP Power (W)	Set Pressure (W)	Forward Power (W)	Chamber Temperature (Deg)	Helium Pressure (Torr)	Time (min)	Deposition thickness (nm)
13	4	1000	2	20	300	8	50	550

Table S10 Recipe 10 for DRIE Bosch Si etching

Step	C_4F_8 Flux (sccm)	SF_6 Flux (sccm)	Forward Power (W)	ICP Power (W)	APC Pressure (mTorr)	Helium Pressure (Torr)	Time (s)	Cycle numbers	Etching Depth (μm)
1 (deposition)	300	10	0	1000	25	10	2		
2 (etching A)	10	200	50	1000	30	10	1.5	35	5.4
3 (etching B)	10	200	30	1000	30	10	1		

Table S11 Recipe 11 for isotropic Si etching by ICP

SF_6 (sccm)	O_2 (sccm)	Set Pressure (W)	Forward Power (W)	ICP Power (W)	Chamber Temperature (Deg)	Helium Pressure (Torr)	Etching Time (min)	Etching Depth (μm)
30	10	6	50	500	25	8	1	1.6

Supplementary Movies

Movie S1 Comparison of bouncing behaviors of water drops on the NDR and MDR surfaces at different *We*.

Movie S2 Comparison of bouncing behaviors of ethylene glycol drops on the NDR and MDR surfaces at *We* ~ 91.

Movie S3 An ethylene glycol drop with *We* up to 306 completely rebounds on the NDR surface.

Movie S4 Comparison of bouncing behaviors of ethanol drops on the NDR and MDR surfaces at *We* ~ 28.

Movie S5 An ethanol drops with *We* up to 57 completely rebounds on the NDR surface.

References

1 A. Cassie, S. Baxter, Wettability of porous surfaces, Trans. Faraday Society, 1944, 40, 546

2 C. Wu, Y. Fan, H. Wang, J. Li, Y. Chen, Y. Wang, L. Liu, L. Zhou, S. Huang, X. Tian, Whether and when superhydrophobic/superoleophobic surfaces are fingerprint repellent, Research, 2022, 2022, 9850316

